Decomposition of Interfacial Crack Driving Forces in Dissimilar Joints

Yun-Jae Kim and
(GKSS Research Center, Institute of Materials Research, Germany)
Hyungyil Lee*
(Sogang University)

This paper presents a framework how to estimate crack driving forces in terms of crack-tip opening displacement and J-integral for mismatched dissimilar joints with interface cracks. The mismatch in elastic, thermal, and plastic hardening properties is not considered, but the mismatch in plastic yield strengths is emphasized here. The main outcome of the present work is that the existing methods to estimate crack driving forces for homogeneous materials can be used with slight modification. Such modification includes (i) mismatch- corrected limit load solutions, and (ii) evaluating the contribution of each material in dissimilar joints to the total crack driving force, which depends on the strength mismatch of the dissimilar joints.

Key Words: Crack Driving Force, CTOD, J-integral, Dissimilar Joint, Strength Mismatch

1. Introduction

Application of fracture mechanics concept to structural assessment procedures requires crack driving force estimates in terms of either crack-tip opening displacement (CTOD) or J-integral. For homogeneous cracked structures, procedures to estimate crack driving forces are well established (ETM, 1997; Kumar *et al.*, 1981).

In many technical areas, two or more dissimilar materials are joined together, either by bonding (solid state) or welding (fusion process) in order to achieve functional requirements, such as metal-metal and metal-ceramic bimaterial joints. For such materials and material systems, interfaces are intrinsic, and the structural performance would be generally limited by fracture along the interface. Thus crack driving force estimates for such dissimilar joints would be necessary for the assessment of the integrity of mechanical structures as well as for the transferability of laboratory test results to structural components. Unlike for homogeneous materials, mismatch in elastic properties as well as plastic properties will affect crack driving forces. Many works have been reported, but mainly concentrate on crack-tip stress fields in either elastic or small scale yielding (Williams, 1959; Symington, 1987; Rice, 1987; Shih and Asaro, 1988, 1989; Shih *et al.*, 1991; Zywicz and Parks, 1989, 1992: Lee *et al.*, 1999).

The present work provides a framework to estimate crack driving forces for mismatched dissimilar joints. Our goals have the following two folds. The first one is to answer whether existing procedures (ETM, 1997; Kumar *et al.*, 1981) could be used with a possible minor modification. For dissimilar joints, this slight modification means that it is be necessary to separate the crack driving force in each material. Thus the second goal is to provide a rule to separate the driving force.

* Corresponding Author,
E-mail : hylee@ccs.sogang.ac.kr
TEL : +82-2-705-8636 ; **FAX** : +82-2-712-0799
Department of Mechanical Engineering, Sogang University, 1, Sinsu-dong, Mapo-gu, Seoul 121-742 Korea.
(Manuscript Received April 27, 1999 ; Revised August 28, 1999)

2. Assumption and Analysis

2.1 Assumption

A bimaterial joint of two elastic-plastic mate-

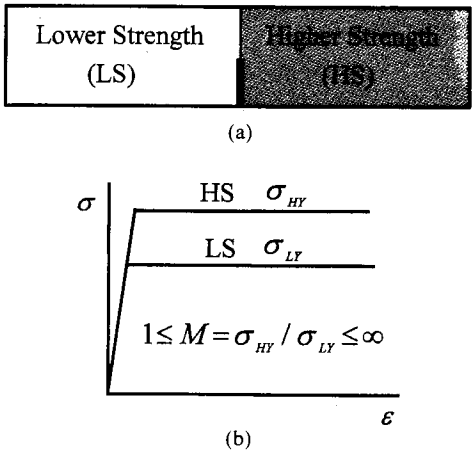

Fig. 1 (a) A mismatched dissimilar joint with an interface crack, and (b) material model assumed in the present work

rials bonded together is considered, with an interface crack lying along the interface of two materials (Fig. 1). Two materials in such dissimilar joints generally have different thermal, elastic, and plastic strength as well as hardening properties. For simplicity, this paper concentrates on two elastic-perfectly plastic materials having the same elastic and thermal properties but different yield strengths, as depicted in Fig. 1. This model both pratically simulates the welding part of low hardening materials and allows distinct analysis of the obtained results. Throughout the paper, the material properties for the lower strength (LS) material and the higher strength (HS) material will be denoted by the subscripts L and H, respectively. The LS material has a yield strength of σ_{LY}, whereas the HS material has of σ_{HY}. The strength mismatch then can be characterized by the mismatch factor M defined as

$$M=\frac{\sigma_{HY}}{\sigma_{LY}}(\geq 1) \tag{1}$$

Note two limiting values of M: $M=1$ corresponds to the homogeneous specimen made of the LS material, and $M=\infty$ to the bimaterial specimen where the HS material is elastic.

The attention is confined here to plane strain conditions and to apparent mode I loading conditions. Note that, even though the apparent loading is mode I, the local crack-tip region can have mixed mode conditions due to the strength mismatch.

2.2 Finite element (FE) analyses

The results given in the subsequent sections were extracted from the 2-D plane strain, elastic-plastic FE analyses where materials were modeled as isotropic elastic-plastic materials which obey nonhardening J_2 flow theory. A small geometry change continuum FE model was employed. To avoid problems associated with incompressibility, 8-node reduced integration elements (element type CPE8R from the ABAQUS library, 1995) were employed. More detailed information on the FE mesh will be given in the corresponding sections.

3. Small Scale Yielding (SSY)

3.1 FE mesh and boundary conditions

The modified boundary layer (MBL) formulation based on the two-term Williams' expansions (Parks, 1992) was employed. Due to elastic homogeneity of bimaterial systems under considerations, the displacement boundary conditions consistent with those for homogeneous materials are applied to the outermost boundary of FE model:

$$u_i=\frac{K_I}{E}\sqrt{\frac{r}{2\pi}}\cdot f_i(\theta,\ \nu)+\frac{T}{E}r\ g_i(\theta,\ \nu) \tag{2}$$

Here E is the Young's modulus and ν is the Poisson's ratio. $f_i(\theta,\ \nu)$ are the angular variations of the elastic singular field, and $g_i(\theta,\ \nu)$ are the angular variations of the displacements due to the T-stress term which is the nonsingular stress acting parallel to the crack flank. The crack-tip is surrounded circumferentially by total forty-eight fans of elements (twenty-four fans each in the upper and the lower part), and the size of the smallest element at the crack-tip is about $0.3\times 10^{-5}R$, where R denotes the radius of the outermost radius of the FE mesh. Results are obtained by systematically varying the values of M and of T, while keeping K_I constant. For all computations, the maximum radius of plastic zone from the crack-tip was not more than $0.2\times 10^{-2}R$, which ensures the SSY conditions.

3.2 Plastic zone

Consider a pure K_I loading (zero T-stress) with varying M. Writing the maximum radius of the plastic zone in each side of the two materials as $(r_p)_L = \Lambda_L (K_I/\sigma_{LY})^2$ and $(r_p)_H = \Lambda_H (K_I/\sigma_{HY})^2$, the effect of M on Λ_L and Λ_H is shown in Fig. 2 (a). In the FE model, the plastic zone in each material was defined as the zone where the equivalent Mises stress σ_e exceeds 99% of the yield strength of the respective material, i.e., $\sigma_e \geq 0.99\ \sigma_{LY}$ and $\sigma_e \geq 0.99\ \sigma_{HY}$, respectively. As M increases, Λ_L increases slightly from ~ 0.15 to ~ 0.18, whereas Λ_H decreases rapidly from ~ 0.15 to 0. Thus the effect of M on plastic zone size is negligible in the LS material but is significant in the HS material.

To investigate the effect of the T-stress, two limiting values of M are considered: $M=1$ and $M=\infty$. The T-stress in the subsequent sections is normalized with respect to σ_{LY},

$$\tau \equiv T/\sigma_{LY} \tag{3}$$

Figure 2(b) compares the dependence of Λ_L on τ for $M=1$ and $M=\infty$. The results suggest that the plastic zone size in the LS material of dissimilar joints remains almost constant regardless of M, while it is dominantly affected by T-stress. Of course, its size in the HS material strongly depends on M, as shown in Fig. 2(a).

3.3 Crack-tip opening displacement (CTOD)

Due to the strength mismatch, the LS material experiences more intensive crack-tip opening than the HS material, which gives an asymmetric crack-tip opening profile. Figure 3(a) shows the variations of CTOD (δ_t) with M for the pure K_I loading (zero T-stress). With increasing M, δ_t

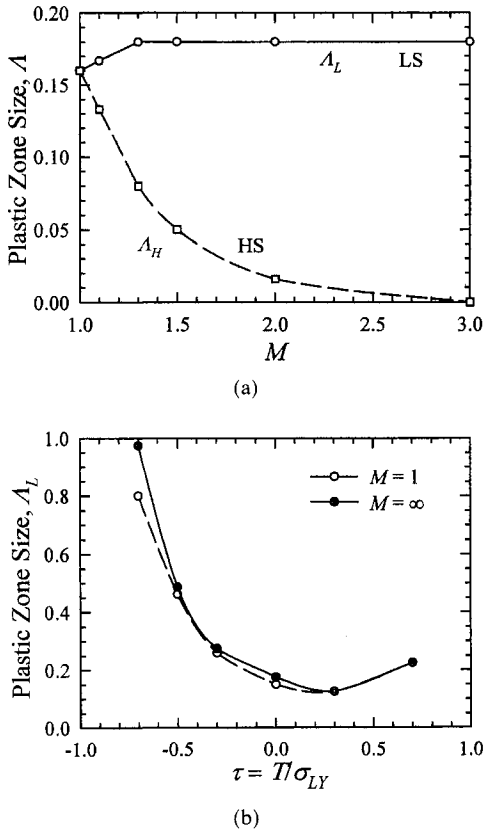

Fig. 2 Variation of plastic zone size with (a) the strength mismatch M and (b) T-stress

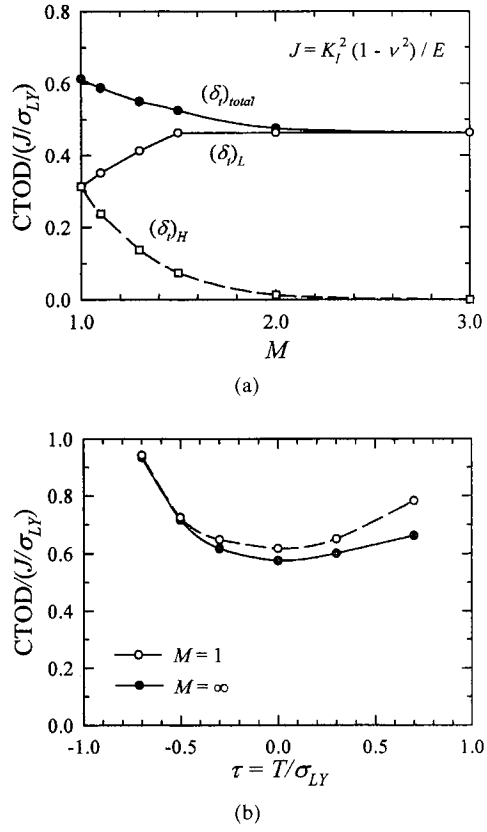

Fig. 3 Variation of crack tip opening displacement with (a) the strength mismatch and (b) T-stress

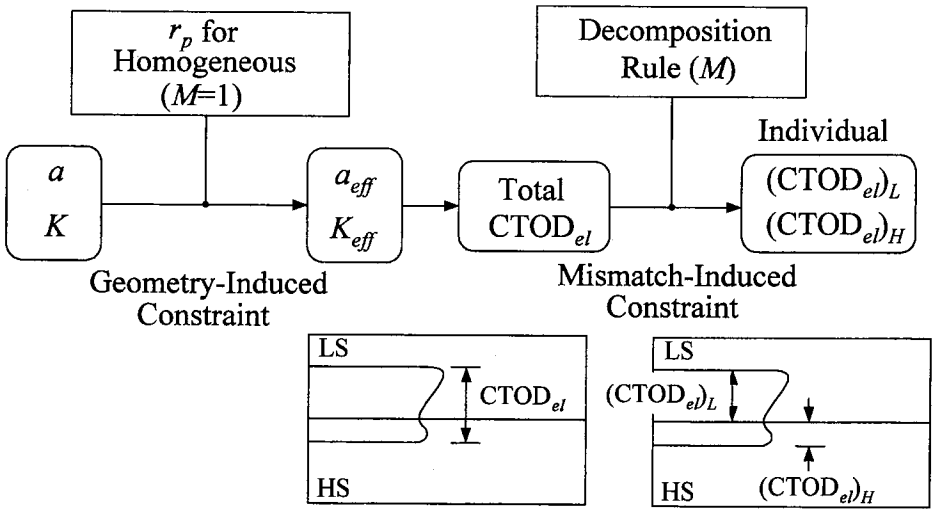

Fig. 4 A framework to estimate crack driving forces for dissimilar joints in SSY

increases in the LS material but decreases in the HS material. One notable point is that, as M increases, δ_t in the LS material increases by up to 50% even though the total δ_t decreases by 25%. Figure 3(b) compares the variations of δ_t with T for bimaterials ($M=\infty$) with those for homoge neous materials ($M=1$). It shows that the magnitudes of δ_t for bimaterials with $M=\infty$ are very similar to those for homogeneous materials ($M=1$).

3.4 Crack driving force estimates in SSY

The results presented in the previous sections provide the strategy to estimate crack driving force in terms of CTOD in SSY, as schematically shown in Fig. 4. For instance, suppose that a crack length a (and the corresponding stress intensity factor K_I) is given for a certain dissimilar joint with the strength mismatch M. Then information on the plastic zone size for homogeneous materials (e.g., see Hauf *et al.*, 1995) can be directly used to determine the plasticity-corrected crack length, a_{eff} and the corresponding stress intensity factor, K_{eff}. Then the elastic component of the CTOD, δ_t^{el}, can be determined from K_{eff}, using the appropriate formula for homogeneous materials. Note that the resulting value of δ_t^{el} is the total value representing the sum of the contributions of the LS and HS materials (Fig. 4).

For dissimilar joints, however, knowledge on the individual contribution of the HS and LS material to δ_t^{el}, $\delta_t^{el}|_H$ and $\delta_t^{el}|_L$ (Fig. 4), would be more relevant. Let's introduce the parameter measuring the relative contribution of the LS material to the total CTOD:

$$\delta = \delta_t^{el}|_L / \delta_t^{el} \tag{4}$$

For instance, when $M=1$, $\delta=0.5$. On the other hand, in the limiting case of $M=\infty$, $\delta=1$. Thus δ should be a function of M. Fig. 5 suggests a form of δ in terms of M. The value of δ increases linearly from 0.5 to 1 for M ranging from 1.0 to 1.8. When $M>1.8$, $\delta\approx 1$ which means that the total CTOD is essentially due to the contribution of the LS material.

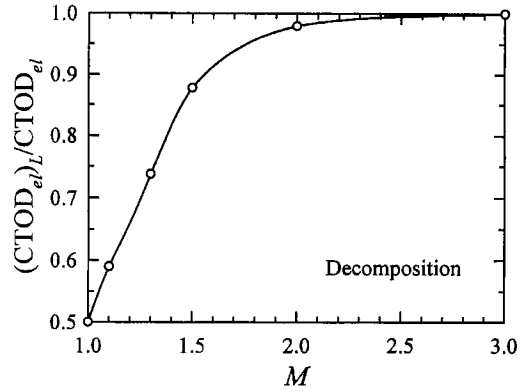

Fig. 5 Contribution of the LS material to the total CTOD

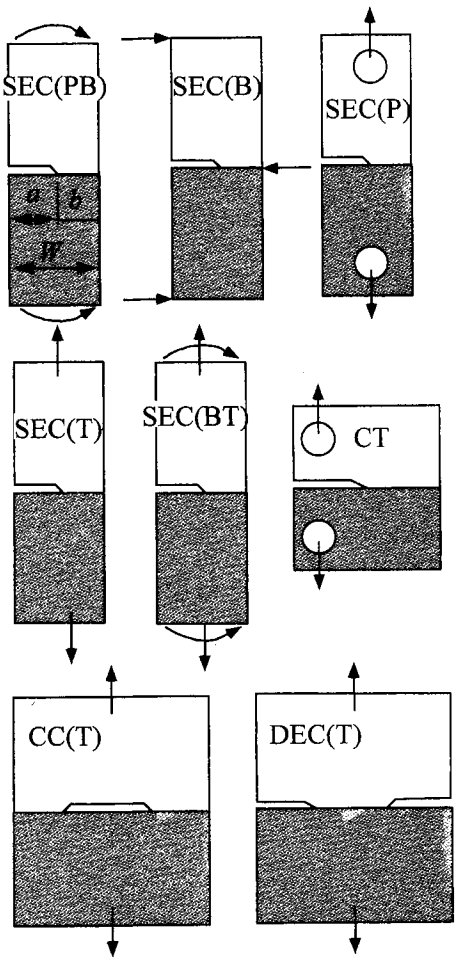

Fig. 6 Plane strain dissimilar specimens considered in this work

4. Full Yielding (FY)

4.1 FE analyses

Eight types of plane strain dissimilar specimens for typical mode I fracture toughness testing are considered here, as depicted in Fig. 6. For a given specimen type, variables investigated are a/W and M. We performed limit analyses of the FE model of bimaterial specimens shown in Fig. 6. Materials were modeled as isotropic elastic-plastic materials which obey nonhardening J_2 flow theory. A small geometry change continuum FE model was employed. The number of elements and nodes in the typical FE mesh ranges about 1000 to 1600 elements and 3100 to 5000 nodes,

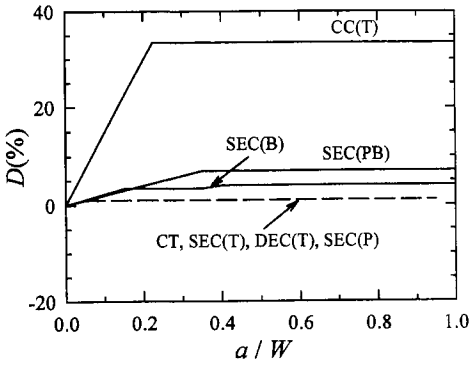

Fig. 7 Variation of $D(\%)$ with a/W for various mismatched dissimilar joints. For the definition of $D(\%)$, see the text

depending on a/W. In all cases, deformation boundary conditions are applied to the FE model, and the magnitude of the applied deformation is made large enough to bring the specimen to its limiting load state. For all cases considered, the FE limit load solutions for homogeneous specimens differ from the known slip line field (SLF) solutions by less than 1%, which provide a confidence of the present FE calculations.

4.2 Limit loads

For homogeneous materials, the limit loads are known for the specimens shown in Fig. 6 (Miller, 1988). The strength mismatch M affects the limit load for dissimilar joints. We introduce the percentage difference of the limit load between dissimilar joints with $M=\infty$ and homogeneous materials $(M=1)$,

$$D(\%)=\frac{F_{YM}(M=\infty)-F_{YM}(M=1)}{F_{YM}(M=1)} \quad (5)$$

where F_{YM} denotes the generalized limit load for dissimilar joints. Figure 7 shows the variation of $D(\%)$ with a/W for various specimens. A remarkable point is that the effect of M on the limit loads is not so significant. For many cases such as C(T), SEC(T) and DEC(T), M does not affect the limit loads at all. For bending specimens such as SEC(B) and SEC(PB), the effect is still slight, *i.e.*, M increases the limit loads but not more than 6%. The most significant effect occurs for CC(T) specimens where M can

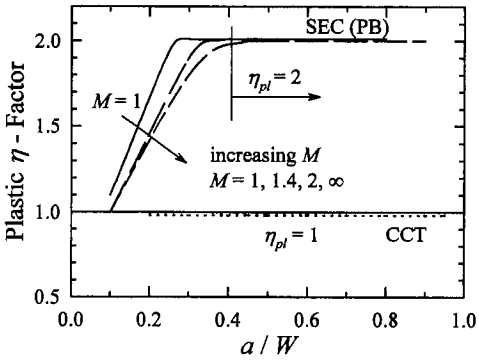

Fig. 8 The effect of the strength mismatch M on the plastic η-factor

increase the limit load by up to 30%. Closed form of limit load solutions for mismatched dissimilar joints in terms of a/W and M are compiled elsewhere (ETM, 1997: Lee and Kim, 1998).

4.3 *J*-Integral and CTOD

The limit load solutions also provide the plastic η-factors, η_{pl}, for determining the plastic component of the J-integral, J^{pl}

$$J^{pl}=\eta_{pl}\cdot\frac{U_{pl}}{B(W-a)} \tag{6}$$

where U_{pl} measures the plastic area under load-load line displacement curve, and B and $(W-a)$ denotes the specimen thickness and the remaining ligament, respectively. According to the load-separation principle, the dependence of η_{pl} on the specimen type and the crack depth can be found from the limit load solutions:

$$\eta_{pl}=-\frac{(W-a)}{P_L}\cdot\frac{\partial P_L}{\partial a} \tag{7}$$

Where P_L denotes the limit load being a function of a/W. Figure 8 shows the variation of η_{pl} with a/W for two typical specimens, CC(T) and SEC (PB), with various values of M. The results in Fig. 8 suggest that the effect of M on η_{pl} is negligible, particularly for deep cracks ($0.45 \leq a/W \leq 0.55$). Thus, as far as the testing method is concerned, the J-integral evaluation procedures for homogeneous specimens can be directly used for any dissimilar joints.

However, due to the strength mismatch, it is not difficult to imagine that the contribution of each material in dissimilar joints to J^{pl} is not equal.

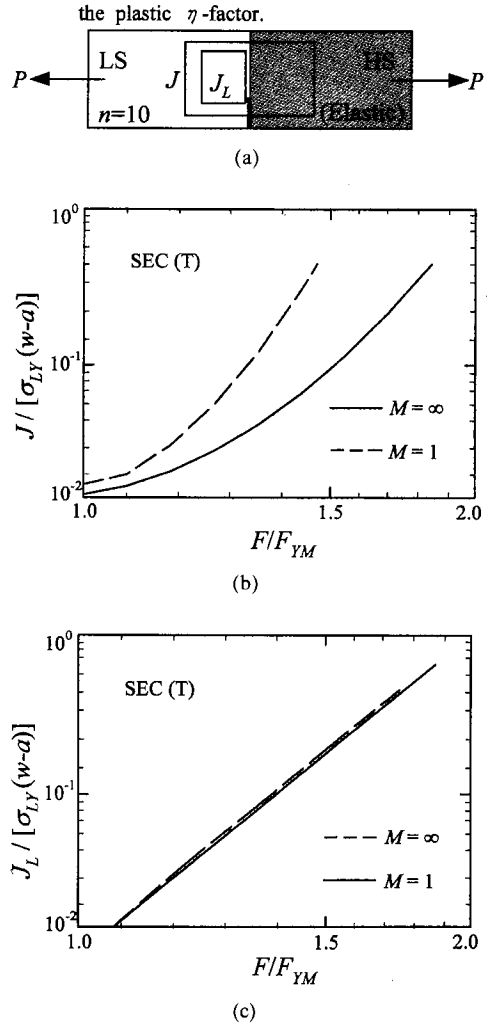

Fig. 9 Variation of the J-integral for mismatched dissmilar SEC(T) speciments

Such fact can be most vividly visualized from Fig. 9 where the J-integrals extracted from the FE analysis of a bimaterial with hardening exponent $n=10$ joined to the elastic material are compared for two limiting SEC(T) dissimilar joints: $M=1$ and $M=\infty$. In the FE analysis, two different contours for the J-integral, J and J_L, were employed, as shown in Fig. 9(a). Note that J reflects the total J-integral whereas J_L does the contribution of the LS material. As shown in Fig. 9(b), when one looks at the total J value, increasing M provides a shielding effect, i.e., for a given load, the J-integral decreases as M increases. However, when the J-integral only in the LS

material, J_L, is looked at, it is not a function of M (Fig. 9(c)). This provides an important key to estimate crack driving forces for dissimilar joints in full yielding.

4.4 Separation of J-Integral and CTOD

In the previous sections, it was suggested that separation of the crack driving force may provide meaningful results. Again, introduce two parameters, $\delta_t|_L/\delta_t$ and J_L/J, measuring the relative contribution of the LS material (Fig. 10). It is obvious that, when $M=1$, $\delta_t|_L/\delta_t=J_L/J=0.5$. On the other hand, in the limiting case of $M=\infty$, $\delta_t|_L/\delta_t=J_L/J=1$. Thus $\delta_t|_L/\delta_t$ and J_L/J should be a function of M. Figure 11 suggests a form of $\delta_t|_L/\delta_t$ and J_L/J in terms of M. For tension loading, the values of $\delta_t|_L/\delta_t$ and J_L/J increases almost linearly from 0.5 to 1 for M ranging from 1 to 2. When $M>2.0$, $\delta_t|_L/\delta_t$ and $J_L/J=1$ which means that the total CTOD is essentially due to the contribution of the LS material. For bending loading, the values of $\delta_t|_L/\delta_t$ and J_L/J sharply increases from 0.5 to 1 for M ranging from 1.0 to 1.2. When $M>1.2$, $\delta_t|_L/\delta_t$ and $J_L/J\approx 1$ which means that the total CTOD is essentially due to the contribution of the LS material.

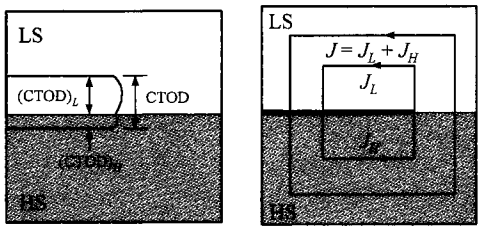

Fig. 10 Schematic illustration of separation of crack driving forces

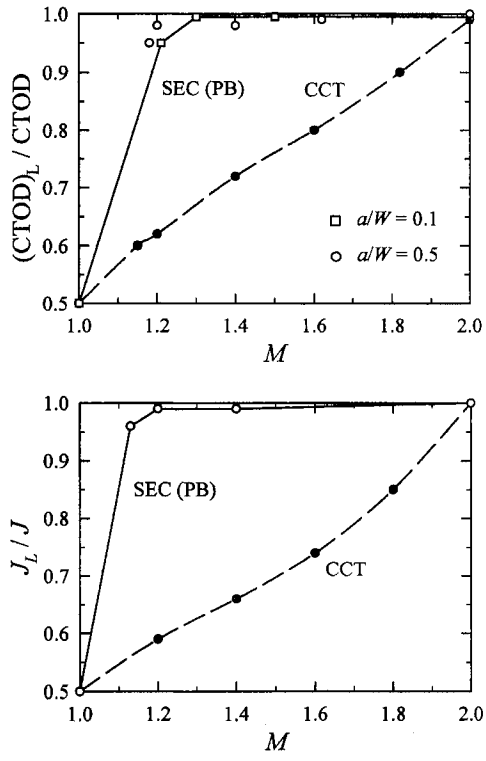

Fig. 11 A framework to separate the crack driving forces for mismatched dissimilar joints in FY

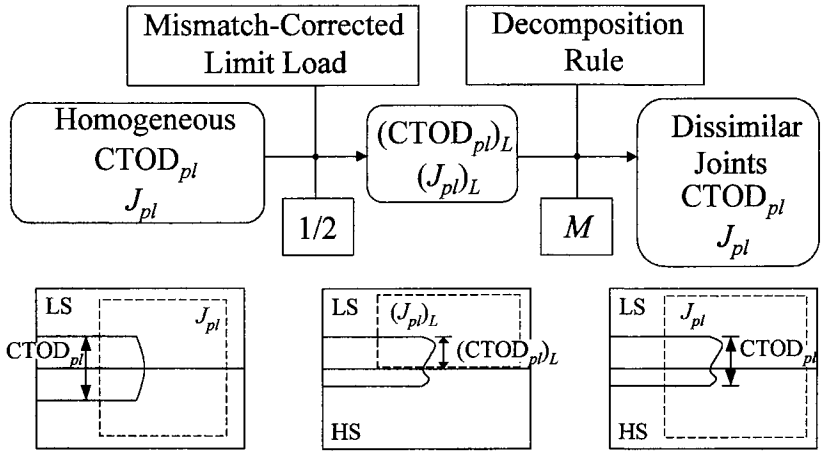

Fig. 12 A framework to estimate crack driving forces for mismatched dissimilar joints in FY

4.5 Crack driving force estimates in FY

The results presented in the previous sections provide the strategy to estimate crack driving force in FY, as schematically shown in Fig. 12. For instance, suppose a dissimilar joint is given. We can obtain driving forces based on the procedures for homogeneous materials made of the LS material. Of course, in this stage, we have to use the mismatch-corrected limit loads presented in Sec. 4.2. The half of the obtained driving forces are those for the LS material. To obtain the total magnitude of the driving forces, he uses the separation rule (Fig. 11) which is a function of M.

5. Conclusions

This paper presents the strategy for estimating crack driving forces for mismatched dissimilar joints, in terms of the CTOD and J-integral. The main outcome of the present work is that the existing methods to estimate crack driving forces for homogeneous materials, such as Engineering Treatment Model (ETM) or EPRI, can be used with slight modification. Such modification includes (i) mismatch-corrected limit load solutions, and (ii) evaluating the contribution of each material in dissimilar joints to the total crack driving forces which depends on the strength mismatch of the dissimilar joints.

Detailed formulations to evaluate crack driving forces are not given in the present work, which can be found easily (ETM, 1997; Kumar *et al.*, 1981). Moreover, the present work did not consider the mismatch in elastic and thermal properties. It is sufficient to say at the moment that such mismatch affects the crack driving forces only in small scale yielding, but not in full yielding. The effect of elastic and thermal mismatch on stress intensity factors has been discussed by O' Dowd *et al.* (1992). Some aspects of the effect of thermal mismatch has been also discussed by Dreier and Schmauder (1993).

Acknowledgments

The authors are grateful for the support provided by a grant from the Korea Science & Engineering Foundation, and Safety and Structural Integrity Research Center.

Reference

ABAQUS *User's Manual*, 1995, Version 5.5, Hibbitt, Karlsson and Sorensen, Inc., Pawtucket, RI.

Dreier, G. and Schmauder, S., 1993, "T-Stress Related to Thermal Residual Stresses in Bimaterials," *Scripta Metallurgica et Materialia,* Vol. 28, pp. 103~108.

EFAM ETM 97: The ETM Method for Assessing the Significance of Crack-Like Defects in Engineering Structures, GKSS Report.

Hauf, D. E., Parks, D. M. and Lee, H., 1994, "A Modified Effective Crack Length Formulation inin Elastic-Plastic Fracture Mechanics," *Mechanics of Materials*, Vol. 20, pp. 273~289.

Lee, H., Ham, J. and Kim, Y-J, 1999, "MBL Based Investigations of Interfacial Crack-Tip Constraint and J-integrals in Plastically Harden ing Bimaterials," *KSME Jounal* A, Vol. 23, No. 9, pp. 1525~1535.

Lee, H. and Kim, Y-J, 1998, "Effect of Strength Mismatch on Fully Plastic Fields in Dissimilar Joints under Combined Loading," *KSME International Journal*, Vol. 12, No. 4, pp. 553-564.

Kumar, G. D., German, M. D. and C. F. Shih, 1981, EPRI: An Engineering Approach for Elastic-Plastic Fracture, EPRI Report NP 1931.

Miller, A. G., 1988, "Review of Limit Loads of Structures Containing Defects," *International Journal of Pressure Vessel and Piping*, Vol. 32, pp. 197~327.

O'Dowd, N. P., Shih, C. F., and Stout, M. G., 1992, "Test Geometries for Measuring Interfacial Fracture Toughness," *International Journal of Solids and Structures*, Vol. 29, pp. 571~589.

Parks, D. M., 1992, "Advances in Characterization of Elastic-Plastic Crack-Tip Fields," in *Topics in Fracture and Fatigue*, (McClintock Festschrift)., Springer-Verlag, 59~98.

Rice, J. R., 1988, "Elastic Fracture Mechanics Concepts for Interfacial Cracks," *Journal of Applied Mechanics*, Vol. 55, pp. 98~103.

Shih, C. F. and Asaro, R. J., 1988, "Elastic-

Plastic Analysis of Cracks on Bimaterial Interfaces: Part I-Small-Scale Yielding," *Journal of Applied Mechanics*, Vol. 55, pp. 299~316.

Shih, C. F. and Asaro, R. J., 1989, "Elastic-Plastic Analysis of Cracks on Bimaterial Interfaces: Part II-Structures of Small-Scale Yielding Fields," *Journal of Applied Mechanics*, Vol. 56, pp. 763~779.

Shih, C. F. and Asaro, R. J. and O'Dowd, N. P., 1991, "Elastic-Plastic Analysis of Cracks on Bimaterial Interfaces: Part III-Large Scale Yielding," *Journal of Applied Mechanics*, Vol. 58, pp. 450~463.

Symington, M. F., 1987, "Eigenvalues for Interface Cracks in Linear Elasticity," *Journal of Applied Mechanics*, Vol. 54, pp. 973~974.

Williams, M. L., 1959, "The Stresses Around a Fault or Crack in Dissimilar Media," *Bulletin of the Seismological Society of America*, Vol. 49, pp. 199~204.

Zywicz, E. and Parks, D. M., 1989, "Elastic Yield Zone Around an Interfacial Crack-Tip," *Journal of Applied Mechanics*, Vol. 56, pp. 577~584.

Zywicz, E. and Parks, D. M., 1992, "Small-Scale Yielding Interfacial Crack-Tip Fields," *Journal of the Mechanics and Physics of Solids*, Vol. 40, pp. 511~536.